# Photon Scanning Tunneling Microscopy Images of Optical Excitations of Fractal Metal Colloid Clusters

D. P. Tsai,[1] J. Kovacs,[1] Zhouhang Wang,[1] Martin Moskovits,[1] Vladimir M. Shalaev,[1,*] J. S. Suh,[2] and R. Botet[3]

[1]*Department of Chemistry and Ontario Laser and Lightwave Research Centre, University of Toronto, Toronto, Ontario, Canada M5S 1A1*

[2]*Department of Chemistry Education, Seoul National University, Seoul 151-742, Korea and Center for Molecular Science, 373-1, Kusung-dong, Taejon 305-701, Korea*

[3]*Laboratoire de Physique des Solides, Université Paris-Sud, Centre d'Orsay, 91405 Orsay CEDEX, France*

(Received 27 July 1993)

Highly localized, laser-excited optical modes of silver colloid fractal clusters were observed using photon scanning tunneling microscopy. The spatial distribution of the modes shows the frequency and polarization selectivity suggested by numerical simulations. The results verify the main concepts of the recently developed resonant optical theory of fractal objects.

PACS numbers: 81.40.Tv, 64.60.Ak, 78.30.Ly, 82.70.Dd

The localization of dynamical excitations in disordered systems and, specifically, in fractal objects is a universal property which plays important roles in many physical processes [1–5]. In particular, localization of resonant dipolar eigenmodes can lead to a dramatic enhancement of many optical effects in fractals [6]. The scaling theory of optical properties of fractals developed in Refs. [7–12] predicts, in particular, that dipolar eigenmodes of fractal clusters are localized in regions smaller than the wavelength [7,10] and can, therefore, concentrate electromagnetic energy in areas smaller than the diffraction limit of conventional optics. This localization of optical excitations can account for the very high local fields leading to the huge enhancement of resonant Rayleigh, Raman, and, especially, of nonlinear light scattering [11–13] observed with colloid clusters of certain metals. In addition to the localization of light-induced dipole excitations fractality can result in the localization (trapping) of the light itself within a range of the order of the wavelength [12]. An important property of the interaction of light with fractals is the very strong frequency and polarization dependence of the spatial location of the light-induced dipole modes. In this Letter, we present numerical simulations and direct experimental observation by means of photon scanning tunneling microscopy (PSTM) of the localization of optical modes in silver colloid fractal clusters.

By operating in the near zone of the dipole fields PSTM can overcome the traditional diffraction limit thereby imaging details smaller than the wavelength [14]. Optical excitations of fractal aggregates can be observed with PSTM by placing the clusters in the evanescent field of a laser beam totally internally reflected in a glass prism.

The PSTM operates by scanning an aperture-limited, optical fiber tapered to a tip with radius of the order of a few tens of nanometers within the near zone of the electromagnetic field radiated by an illuminated sample. For the purpose of simulation we will make the simplifying assumption that the signal detected by the tapered optical fiber tip of the PSTM is proportional to the squared modulus of the local field which is the sum of (i) the evanescent field of amplitude $E_\alpha^{(0)}e^{-\alpha z}$ and (ii) the fields of the dipoles $d_\alpha^{(i)}=\chi_{\alpha\beta}^{(i)}E_\beta^{(0)}e^{-\alpha z_i}$ induced in the particles forming the cluster. The inverse decay length of the evanescent field along the normal to the surface $z$ is $\alpha=2\pi(n^2\sin^2\theta-1)^{1/2}/\lambda$ (not to be confused with the subscript $\alpha$). Here $\lambda$ is the vacuum wavelength of the light, $n$ the refractive index of the prism, and $\theta$ the incident angle.

A general expression for the intensity of a collection of dipoles (assumed to arise from an assembly of polarizable colloidal metal particles) in an evanescent field is given by

$$I(x,y,z)=\left|E_\alpha^{(0)}e^{-\alpha z}-\sum_j V_{\alpha\beta}^{(tj)}\chi_{\beta\gamma}^{(j)}E_\gamma^{(0)}e^{-\alpha z_j}\right|^2, \quad (1)$$

where

$$V_{\alpha\beta}^{(tj)}=\frac{a^{(tj)}\delta_{\alpha\beta}-3b^{(tj)}n_\alpha^{(tj)}n_\beta^{(tj)}}{r_{tj}^3}\exp(ikr_{tj}-ikr_{tj}), \quad (2a)$$

$$a^{(tj)}=1-ikr_{tj}-(kr_{tj})^2,\quad b^{(tj)}=1-ikr_{tj}-(kr_{tj})^2/3, \quad (2b)$$

and $\mathbf{r}_{tj}\equiv\mathbf{r}_t-\mathbf{r}_j$ is the vector connecting the fiber tip and the $j$th particle, $\mathbf{k}$ is the wave vector, and $\mathbf{n}^{(tj)}\equiv\mathbf{r}_{tj}/r_{tj}$. The polarizability of the $j$th particle $\chi_{\beta\gamma}^{(j)}$ in (1) must include the effect of the dipole-dipole interaction among all particles in the aggregates. The operator describing this interaction is given by (2) when $t$ is replaced by $i$, referring to the $i$th particle. It was shown in Ref. [11] that for strongly localized modes on fractals, this operator can be reduced to its Hermitian, near-zone counterpart with

$$a\simeq b\simeq 1,\quad \exp(ikr_{tj}-ikr_{tj})\simeq 1$$

if $kr_{ij}<1$ and $V=0$, otherwise.

A numerical simulation of the intensity distribution, $I(x,y,z=z_0)$ [Eqs. (1) and (2)], of the local fields due to the excitation of dipole eigenmodes on fractal aggregates was carried out as follows. A three-dimensional cluster of 512 particles (i.e., $N=512$) was generated, assuming cluster-cluster aggregation [15] [$N=(R_c/R_0)^D$ where

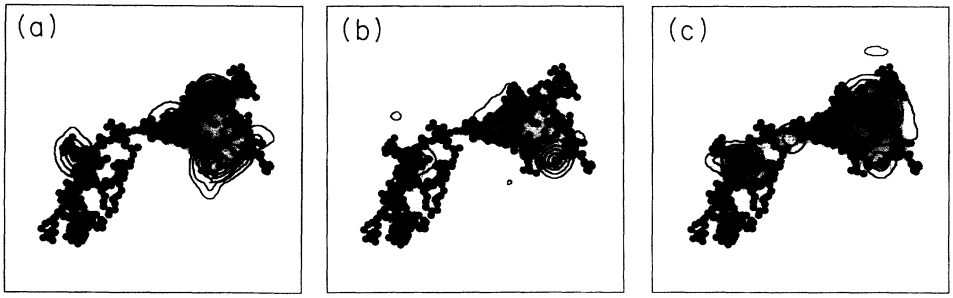


FIG. 1. Computed local field intensity, $I(x,y)$, of the light-induced dipole modes calculated for a fractal aggregate. (a),(b) $X=-0.1$, $s$ and $p$ polarizations, respectively; (c) $X=-0.25$, $s$ polarization.

$D=1.78$ is the fractal dimension, $R_c$ and $R_0$ are, respectively, the radius of gyration of the cluster and a constant of the order of the separation between monomers.] The cluster was then collapsed to its two-dimensional projection, simulating closely the experimental situation. The dipole excitations and local field values were calculated from solution of the $3N$ equations describing the light-induced dipole moments of the particles forming the cluster. The reduced, near-zone operator of the interaction was used and the following parameter values assumed: $\delta \equiv -R_0^3 \mathrm{Im}\chi_0^{-1}=0.01$, $z/R_m=2$ where $R_m$ is the radius of particles, $\chi_0$ the polarizability of an isolated particle, and $\lambda/R_m=50$. This corresponds approximately to the experimental situation for which $R_m \simeq 10$ nm and $\lambda \simeq 500$ nm. The constant $\delta$ expresses the dielectric losses. The quantity $X \equiv -R_0^3 \mathrm{Re}\chi_0^{-1}$ plays the role of a spectral variable such that $X=0$ at resonance ($\omega=\omega_0$) and $X \propto \omega-\omega_0$ in the vicinity of the resonance, for an isolated particle. For a cluster composed of colloidal metal particles the resonance is associated with localized surface plasmon (LSP) oscillations.

Figure 1 shows $I(x,y)$ calculated at two values of the photon energy and for both $s$ and $p$ polarizations. The localization of the modes is clearly visible. This differs from the situation expected for a compact aggregate ($D=3$) where the effect of the dipole-dipole interaction is long ranged and the normal modes would, therefore, be delocalized over the entire cluster. The linear dimension of the high local field regions in Fig. 1 varies from mode to mode. On average, a mode spans several tens of nm when $R_m=10$ nm. The frequency and polarization sensitivity of the mode localization is evident in Fig. 1: A change in either the frequency of light (parameter $X$) or polarization results in the excitation of new resonant modes with different spatial locations and intensities.

The scale invariance of fractal clusters resulting from cluster-cluster aggregation of colloid particles is statistical. Spatial localization of light-induced dipole modes and their sensitivity to polarization and frequency should also be observed on geometrically ordered fractals. Figure 2 shows $I(x,y)$ for a Vicsek cluster, computed using parameters similar to those used previously to generate Fig. 1 except that $\lambda/R_m=25$. Again, strong localization of the optical excitations is evident. Interestingly, there is no symmetry in the positions of the light-induced eigenmodes despite the high symmetry of the Vicsek fractal. The symmetry breaking results from the incommensurate structure of the light field with respect to that of the cluster. Specifically it is the introduction of the two vectors, $\mathbf{E}^{(0)}$,$\mathbf{k}$, together with the tensor character of the dipole-dipole interaction that breaks symmetry.

The experimental search for localized electromagnetic excitations on fractal clusters was carried out as follows. A right-angle BK-7 glass prism was illuminated normal to one of the small faces resulting in total internal reflection at the hypotenuse face. Measurements were carried out with 20 mW of unfocused argon-ion laser light ($\lambda=488$ and 514.5 nm).

Gold-coated tapered fiber tips [16] with effective optical apertures of 20 to 50 nm were mounted in a piezoelectric tube scanner with a maximum scanning area of 9 $\mu$m$\times$9 $\mu$m. The light output from the fiber was detected with a cooled photomultiplier.

Images were normally recorded in the constant intensity mode. That is, the $z$ position of the tip was piezoelectrically adjusted by means of feedback electronics so as to keep the photomultiplier output constant at a value $I_s$. The control voltage delivered to the piezo tube, which is proportional to the tube displacement, was displayed as a function of $x,y$.

Fractal aggregates of silver colloid particles were produced from a silver sol generated by reducing silver nitrate with sodium borohydride [17]. Addition of an adsorbate (phthalazine) promotes aggregation, in this case

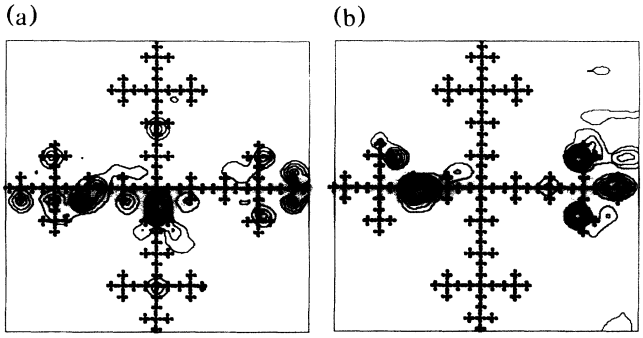


FIG. 2. Computed local field intensity, $I(x,y)$, of the light-induced dipole modes on a Vicsek fractal. (a),(b) $s$ polarization, $X=-0.1$ and $-0.25$, respectively.

forming fractal colloid clusters having fractal dimension approximately equal to 1.78 [18]. Clusters were allowed to settle slowly out of solution onto Pyrex microscope cover slides for PSTM measurements and for scanning electron microscopy (SEM) imaging. SEM images clearly show the fractal structure of the aggregates. The average cluster was several microns in size. Index matching oil was used to mount the microscope slide to the prism.

Before proceeding further, it is instructive to consider how the optical modes will be imaged by the PSTM. The local fields due to the resonant dipole modes are significantly more intense than the external evanescent field. The quality factor $Q$ characterizes the corresponding enhancement [6,7,11]. Accordingly, for resonant eigenmodes the second term in Eq. (1) is of the order of $QE^{(0)}$ ($e^{-\alpha z_j} \simeq 1$). It is convenient to separate the contributions to the quantity $I(x,y)$ as given in (1) into three parts: A background signal $|E^{(0)}e^{-\alpha z}|^2$, the interference part, $\sim |E^{(0)}|^2 e^{-\alpha z} Q \exp[ikr_{tj} - ikr_{tj}]$, and the largest contribution, $\sim |E^{(0)}Q|^2$, due to the excitation of resonant fractal modes. The dipole eigenmodes are characterized by a spatial localization dimension, $l_x$. The field associated with an excited mode for which $l_x < \lambda$ decreases as $r^{-3}$ in the region $r > l_x$ ($r$ is the distance from the mode center to the point of observation) so that the corresponding intensity, $I(r)$, decreases as $r^{-6}$. Thus

$$I(r) \simeq \begin{cases} I_0 \text{ for } r \le l_x, \\ I_0 (l_x/r)^6 \text{ for } r > l_x, \end{cases}$$

where $I_0 \simeq Q^2 |E^{(0)}|^2$ is the (enhanced) intensity at the center of the excited mode. These approximations regarding $I(r)$ are valid for $r$ up to $-\lambda$.

In regions of the surface devoid of resonant modes, the tip of the PSTM operating in the constant intensity mode will be positioned a distance $z$ above the surface such that $I_s \simeq |E^{(0)}e^{-\alpha z}|^2$. When an excited mode is approached, the tip will move along a bell-shaped surface defined by $I(r) = I_s$ which is characterized, at half its maximum height, by a radius $R_x$ such that $Q^2 (l_x/R_x)^6 \simeq 1$. (Recall that $e^{-\alpha z} \sim 1$ in the "dark" region far from a resonant mode.) The image of an eigenmode with localization length $l_x$ will, therefore, be magnified by the PSTM so that its characteristic radius is approximately $R_x \simeq Q^{1/3}$

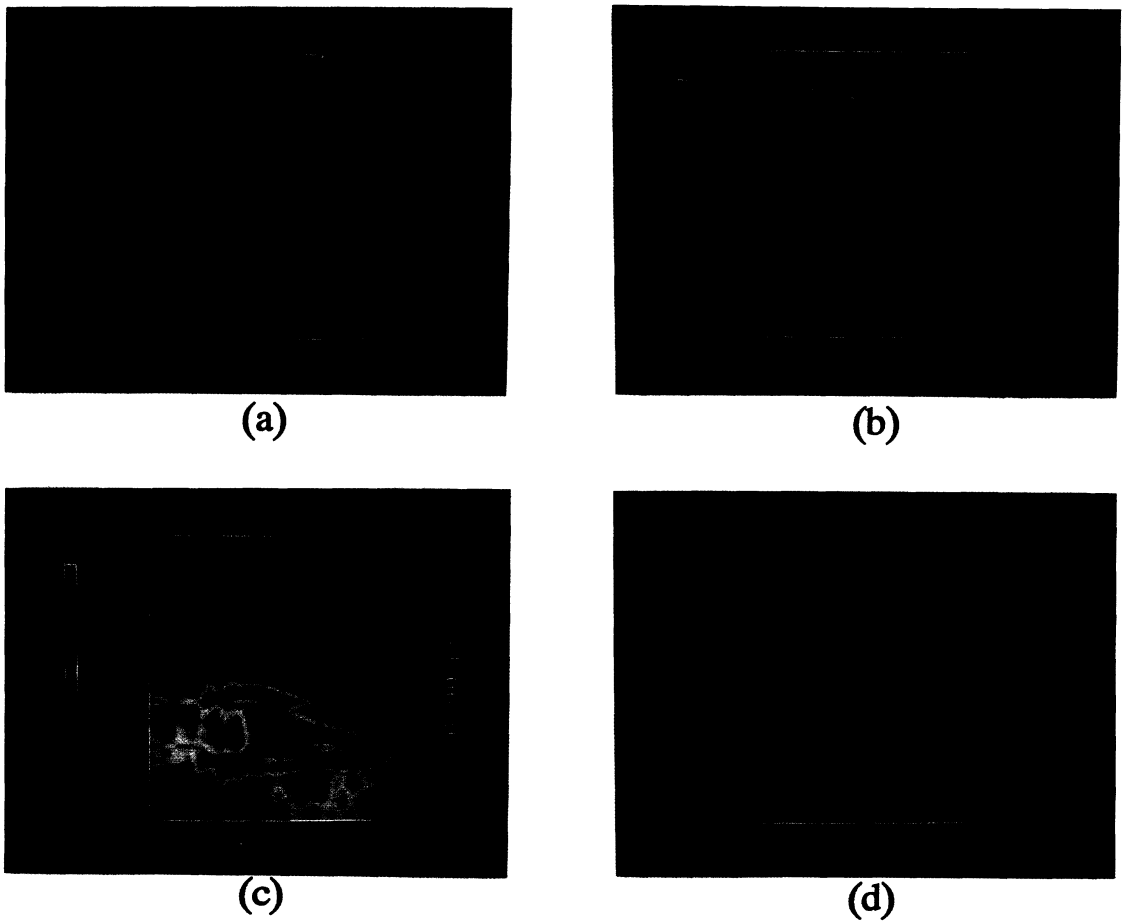


FIG. 3. Photon STM images of local fields in fractal silver colloid aggregates irradiated by light of varying wavelength and polarization. (a),(b) $\lambda = 488$ nm, $s$ and $p$ polarizations, respectively; (c),(d) $p$ polarization, $\lambda = 488$ and 514.5 nm, respectively. Two different samples were used to obtain images (a),(b) and images (c),(d).

$\times l_x$. For silver with $Q \simeq 10^2$, $R_x \simeq 5 l_x$. Hence in PSTM images, the lateral dimensions of excited dipole eigenmodes of silver colloid clusters are expected to be larger than $l_x$ by approximately a factor of 5.

Photon STM images of fractal colloidal silver aggregates recorded at two different wavelengths and with both $s$ and $p$ polarizations are shown in Fig. 3. The images were highly reproducible. The images shown in the figure bear many similarities with those simulated numerically. In particular, they indicate highly localized "hot spots" as well as the expected sensitivity of the spatial location of these high intensity spots to frequency and polarization. Accordingly we identify them with the highly localized dipolar LSP eigenmodes of the fractal cluster. The radii of the images of the excited optical eigenmodes, $R_x$, are measured to range from 300 to 700 nm, implying that the localization length $l_x$ lies in the range 60 to 140 nm in agreement with the results of the numerical simulations. The interference fringes which arise from the term $\propto \exp[ikr_{tj} - ikr_{tj}]$ in (1) are also clearly visible.

Control experiments performed with cover slips on which no fractal clusters were deposited confirmed that the images shown in Fig. 3 arise from colloidal aggregates. The color scale used to indicate the height of the tip above the surface shows that at the "hot spots" the tip retracts to a height $z_{\max} \simeq 400$ to 600 nm above its value in the dark regions of the image. In control experiments the tip retraction was never above 200 nm. Such a dramatic increase in the tip height (recall that the evanescent field intensity decreases exponentially, while the field intensity due to the resonant modes as $r^{-6}$) implies a very strong field enhancement in the vicinity of the hot spots strongly suggesting that these intense features are the resonant modes discussed above. Moreover, we concluded above that $R_x$ would be significantly larger than $l_x$ for a PSTM image obtained in the constant intensity mode. Since in the observed image $R_x \sim \lambda$, one concludes that $l_x$ is significantly smaller than the wavelength. This justifies the assumption that $l_x < \lambda$ in the analysis outlined above and the corresponding estimates based on this assumption.

We, therefore, conclude that the strong spatial localization and the frequency and polarization dependence of the resonant eigenmodes of fractal silver colloid clusters have been successfully observed using PSTM verifying the seminal predictions regarding the resonant optics of fractals reported in [7,10–13].

The authors are grateful to C. Douketis and A. Rovinsky for useful discussions. Financial support from NSERC and CEMAID is also gratefully acknowledged.

*Present address: Department of Physics, New Mexico State University, Las Cruces, NM 88003.

[1] S. Alexander and R. Orbach, J. Phys. (Paris), Lett. **43**, L625 (1982); R. Rammal and G. Toulouse, J. Phys. (Paris), Lett. **44**, L13 (1983); R. Bourbonnais, R. Maynard, and A. Benoit, J. Phys. (Paris) **50**, 3331 (1989).

[2] B. Sapoval, Th. Gobron, and A. Margolina, Phys. Rev. Lett. **67**, 2974 (1991).

[3] A. Bunde, H. E. Roman, S. Russ, A. Ahoroni, and A. B. Harris, Phys. Rev. Lett. **69**, 3189 (1992); M. Schreiber and H. Grussbach, Phys. Rev. Lett. **67**, 607 (1991).

[4] A. Petri and L. Pietronero, Phys. Rev. B **45**, 12864 (1992); F. Craciun, A. Bettucini, E. Molinari, A. Petri, and A. Alippi, Phys. Rev. Lett. **68**, 1555 (1992); M. Montagna, O. Pilla, G. Viliani, V. Mazzacurati, G. Ruocco, and G. Signorelli, Phys. Rev. Lett. **65**, 1136 (1990).

[5] *Fractals & Disorder*, edited by Armin Bunde (North-Holland, Amsterdam, 1992).

[6] V. M. Shalaev and M. I. Stockman, Zh. Eksp. Teor. Fiz. **92**, 509 (1987) [Sov. Phys. JETP **65**, 287 (1987)]; Z. Phys. D **10**, 71 (1988); A. V. Butenko, V. M. Shalaev, and M. I. Stockman, Zh. Eksp. Teor. Fiz. **94**, 107 (1988) [Sov. Phys. JETP **67**, 60 (1988)]; Z. Phys. D **10**, 81 (1988).

[7] V. A. Markel, L. S. Muratov, and M. I. Stockman, Zh. Eksp. Teor. Fiz. **98**, 819 (1990) [Sov. Phys. JETP **71**, 455 (1990)]; V. A. Markel, L. S. Muratov, M. I. Stockman, and T. F. George, Phys. Rev. B **43**, 8183 (1991).

[8] K. Ghosh and R. Fuchs, Phys. Rev. B **38**, 5222 (1988); R. Fuchs and F. Claro, Phys. Rev. B **39**, 3875 (1989); F. Claro and R. Fuchs, Phys. Rev. B **44**, 4109 (1991); K. Ghosh and R. Fuchs, Phys. Rev. B **44**, 7330 (1991).

[9] P. M. Hui and D. Stroud, Phys. Rev. B **33**, 2163 (1986); I. Hoffmann and D. Stroud, Phys. Rev. B **43**, 9965 (1991); I. H. H. Zabel and D. Stroud, Phys. Rev. B **46**, 8132 (1992).

[10] M. I. Stockman, T. F. George, and V. M. Shalaev, Phys. Rev. B **44**, 115 (1991); V. M. Shalaev, R. Botet, and A. V. Butenko, Phys. Rev. B **48**, 6662 (1993).

[11] V. M. Shalaev, R. Botet, and R. Jullien, Phys. Rev. B **44**, 12216 (1991); **45**, 7592(E) (1992); M. I. Stockman, V. M. Shalaev, M. Moskovits, R. Botet, and T. F. George, Phys. Rev. B **46**, 2821 (1992); V. M. Shalaev, M. I. Stockman, and R. Botet, Physica (Amsterdam) **185A**, 181 (1992).

[12] V. M. Shalaev, M. Moskovits, A. A. Golubentsev, and S. John, Physica (Amsterdam) **191A**, 352 (1992).

[13] S. G. Rautian, V. P. Safonov, P. A. Chubakov, V. M. Shalaev, and M. I. Stockman, Pis'ma Zh. Eksp. Teor. Fiz. **47**, 243 (1988) [JETP Lett. **47**, 243 (1988)]; A. V. Butenko, P. A. Chubakov, Yu. E. Danilova, S. V. Karpov, A. K. Popov, S. G. Rautian, V. P. Safonov, V. V. Slabko, V. M. Shalaev, and M. I. Stockman, Z. Phys. D **17**, 283 (1990).

[14] E. Betzig and J. K. Trautman, Science **257**, 189 (1992); R. C. Reddick, R. J. Warmack, and T. L. Ferrel, Phys. Rev. B **39**, 767 (1989).

[15] R. Jullien and R. Botet, *Aggregation and Fractal Aggregates* (World Scientific, Singapore, 1987).

[16] D. P. Tsai, Z. Wang, and M. Moskovits, Proc. SPIE Int. Soc. Opt. Eng. **1855**, 93 (1993).

[17] J. A. Creighton, in *Surface Enhanced Raman Scattering*, edited by R. K. Chang and T. E. Furtak (Plenum, New York, 1982).

[18] D. A. Weitz and M. Oliveria, Phys. Rev. Lett. **52**, 1433 (1984).

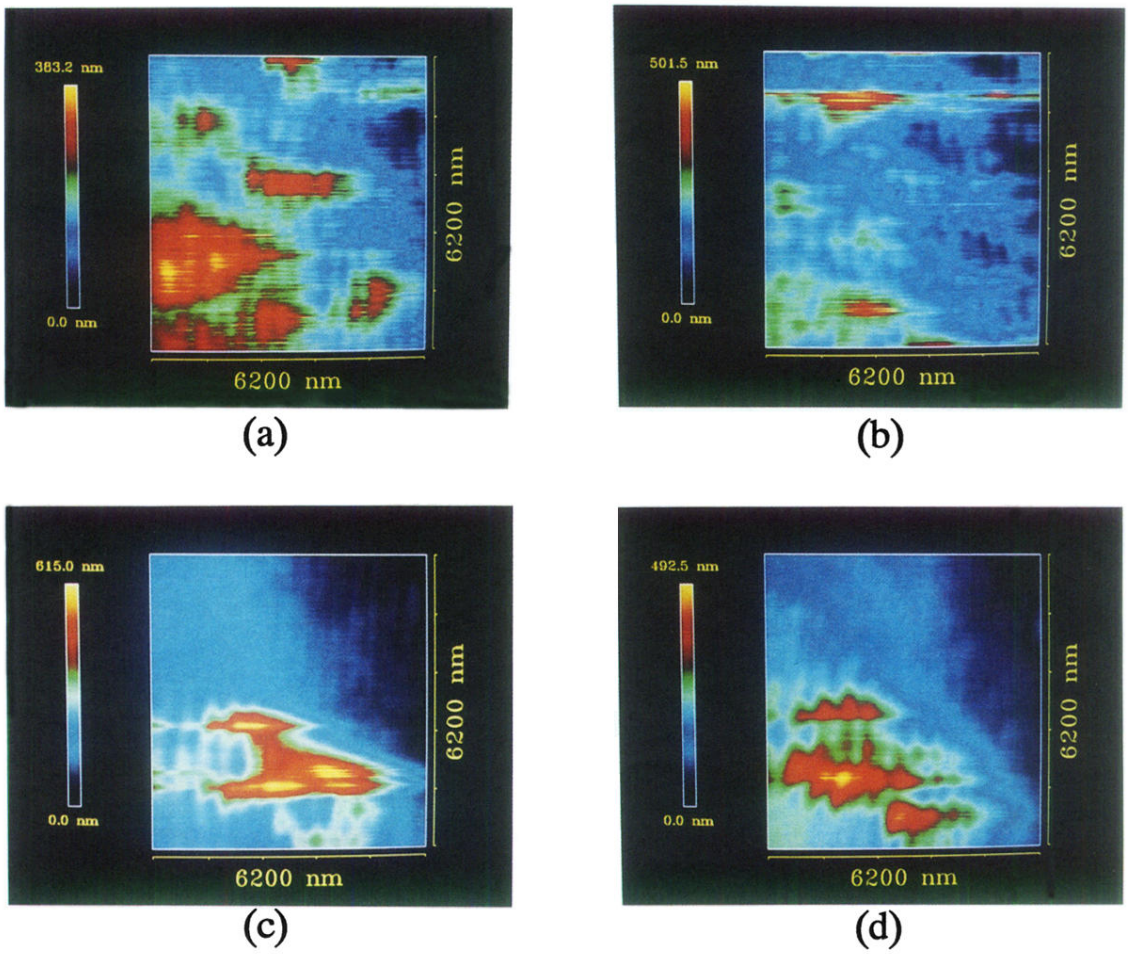


FIG. 3. Photon STM images of local fields in fractal silver colloid aggregates irradiated by light of varying wavelength and polarization. (a),(b) $\lambda = 488$ nm, *s* and *p* polarizations, respectively; (c),(d) *p* polarization, $\lambda = 488$ and 514.5 nm, respectively. Two different samples were used to obtain images (a),(b) and images (c),(d).